NASA Technical Memorandum 107373

Imaging of Combustion Species in a Radially-Staged Gas Turbine Combustor

Randy J. Locke
NYMA, Inc.
Brook Park, Ohio

Yolanda R. Hicks and Robert C. Anderson
Lewis Research Center
Cleveland, Ohio

Kelly A. Ockunzzi
Case Western Reserve University
Cleveland, Ohio

Harold J. Schock
Michigan State University
East Lansing, Michigan

Prepared for the
33rd Joint Combustion and Propulsion Systems
Hazards Subcommittees Meeting
sponsored by the Joint Army-Navy-NASA-Air Force
Interagency Propulsion Committee
Monterey, California, November 4–9, 1996

National Aeronautics and
Space Administration

Imaging of Combustion Species in a Radially-Staged Gas Turbine Combustor

Randy J. Locke
Aeropropulsion Systems Department
NYMA, Inc.
Brook Park, Ohio 44142

Yolanda R. Hicks and Robert C. Anderson
NASA Lewis Research Center
Cleveland, Ohio 44135

Kelly A. Ockunzzi
Computer Engineering Department
Case Western Reserve University
Cleveland, Ohio 44106

Harold J. Schock
Mechanical Engineering Dept.
Michigan State University
East Lansing, Michigan 48864

ABSTRACT

Planar laser-induced fluorescence (PLIF) is used to characterize the complex flowfield of a unique fuel-lean, radially-staged, high pressure gas turbine combustor. PLIF images of OH are presented for two fuel injector configurations. PLIF images of NO, the first acquired at these conditions, are presented and compared with gas sample extraction probe measurements. Flow field imaging of nascent C_2 chemiluminescence is also investigated. An examination is made of the interaction between adjoining lean premixed prevaporized (LPP) injectors. Fluorescence interferences at conditions approaching 2000 K and 15 atm are observed and attributed to polycyclic aromatic hydrocarbon (PAH) emissions. All images are acquired at a position immediately downstream of the fuel injectors with the combustor burning JP-5 fuel.

INTRODUCTION

A significant volume of work has been done to characterize combustion processes in simple gaseous flames by way of measurements of species concentration, temperature, velocity and pressure.[1-3] Until recently, few investigations have been initiated with practical high pressure/high temperature aeropropulsion combustor applications. Principal among these studies is the PLIF examination of heptane-fueled spray flame species[4] at pressures approaching 10 atm, and the imaging study of the high pressure environment of optically accessible reciprocating engines[5] using a tunable excimer KrF laser.

Recently, researchers at NASA Lewis Research Center have used OH PLIF to examine the complex flowfields in single injector flametubes burning JP-5 fuel.[6] These studies were performed in a unique, optically accessible flametube. This device, when coupled with nonintrusive optical diagnostic methods, permits direct measurement of parameters critical to advanced combustor and subcomponent design. Previous diagnostic methods in these large scale rigs employed invasive probe-based measurements that perturbed the flow field, thus adversely affecting the analysis.

The work presented here is an extension of that earlier NASA single injector subcomponent work to a more complex radially-staged gas turbine combustor test rig. Although many optical diagnostics exist for performing in-situ measurements on reacting flows,[7] PLIF was selected for this study due to its ability to

characterize a flow in two dimensions, its species specificity, the degree to which it can be quantified, and the potential to extract planar temperature information. The fluorescence from excited OH, NO and C_2 molecules was acquired at lean burning conditions for a number of fuel injector configurations over a range of pressures (8 atm - 14 atm), inlet temperatures (728 K to 866 K), equivalence ratios (ϕ = 0.41 to 0.59), and air flow rates (1.86 kg/s to 4.10 kg/s).

The OH radical was chosen for study not only because it serves as a reaction zone marker, but also due to its importance as a reaction intermediate. NO was examined because it is a pollutant in lean burning combusting systems, and as such, is a major concern of new aerospace propulsion initiatives.[8-9] A characteristic of combustors is that the local fuel-air distribution fluctuates, giving rise to hot spots that are responsible for the bulk of NO production. Gas probes have provided average NO concentrations but are incapable of providing an in-situ measurement of NO distribution. Planar imaging will address this concern. Finally, C_2 was examined because it too is a fuel marker with the added benefit that it can be visualized without laser excitation, allowing elucidation of the flow in regions inaccessible to lasers. Using the fluorescence from these molecular species, fuel/air mixing, flame structure, and the interaction between adjacent fuel injectors are examined.

We present here the first use of PLIF imaging of flame species to analyze the high pressure, high temperature flow fields encountered in a JP-5 burning, radially-staged gas turbine combustor sector rig.

EXPERIMENTAL HARDWARE AND PROCEDURES

OPTICAL SYSTEM

Wavelengths used in this study to excite the NO $A^2\Sigma^+ \leftarrow X^2\Pi$ (0,0) and OH $A^2\Sigma^+ \leftarrow X^2\Pi$ (1,0) transitions were generated using a Continuum ND 81-C Nd:YAG which pumps a ND-60 dye laser. An ultraviolet wavelength extension (UVX) system provided doubling and mixing after doubling capabilities when pumped by the Nd:YAG second harmonics of 750 mJ/pulse at 10 Hz. For OH excitation the dye laser used a Rhodamine 590 dye solution yielding approximately 185 mJ at 566 nm. Doubling the resultant dye output provided approximately 16 mJ at 283 nm. To achieve NO γ-band excitation, the dye laser used a mixture of 80% Rhodamine 590 and 20% Rhodamine 610 dye solution. The doubled dye output was mixed with residual 1064 nm infrared resulting in laser energy of 4mJ near 225.5 nm. The bandwidth of these wavelengths was 1.0 cm^{-1} as measured by a Burleigh pulsed UV wavemeter. The pulse widths were 7 ns at FWHM. A pellin-broca prism isolated the appropriate UV wavelength from the residual dye and pump fundamental. Excitation wavelength verification was accomplished for OH by splitting off 5% of the prepared UV output and passing it through a Bunsen burner flame at atmospheric pressure. For NO, the UV beam was directed through a high pressure vessel containing 250 ppm NO in argon. The fluorescence from each was monitored with a photo-multiplier/boxcar averager system.

Figure 1 illustrates the optical system used in this series of experiments to deliver the laser beam to the test section. The UV laser beam, possessing a divergence of ~5 mrad, was allowed to freely expand through the optical path that was approximately 82 ft (25 m) in length. Sheet forming was accomplished with a 3000 mm focal length cylindrical lens resulting in a sheet with approximate dimensions of 25 mm x 0.3 mm. Figure 2 shows details of the two configurations used for the final segment of the optical delivery system. Figure 2(a) displays details for horizontal laser sheet insertion, while Figure 2(b) shows details for vertical laser sheet insertion. Also shown in Figure 2 is the ICCD camera detector for both laser sheet input arrangements as well as a beam profiler that was used to monitor laser sheet positioning.

The angular position of all mirrors in the beam transport system is controlled by remote operation. Additionally, mirrors 2-6 are mounted on motorized traversing stages that provide remotely controlled linear motion. Linear movement of the mirrors is necessary in order to reposition the laser sheet across the incident window and consequently to access the entire flowfield within the window field of view. Stream-wise movement of mirrors 4 and 5 is needed to counteract rig growth which has been found to be approximately 5 mm in the upstream direction. Movement of the ICCD camera, mounted either above the

rig for horizontal laser input, or alongside the rig for vertical laser input, is provided by a 2- or 3-axis positioning system. The camera stages act in concert with the laser excitation beam via a custom-designed computer program. This action is required to maintain the camera focus at the laser sheet focal plane. Error in laser sheet placement for the horizontal beam was ± 0.04 in (1 mm); for the vertically inserted beam the error in placement was ± 0.08 in (2 mm).

IMAGE COLLECTION

Detection of the planar fluorescence was accomplished by using a Princeton Instruments gated and intensified charge-coupled device (ICCD) with an array size of 384 x 576 pixels. The camera intensifier was synchronously triggered with the laser pulse through a Princeton Instruments FG-200 pulse generator. A Princeton Instruments ST-100 detector controller was used to provide a gating period of 75 ns. The planar fluorescence normal to the laser excitation sheet was collected through a 105 mm Nikon f/4.5 UV Nikkor lens. Princeton Instrument's Winview software package was used to acquire all images. Elimination of noise (e.g., scattered laser light, non-resonant excitation, radiation from the combustor walls and from the self luminous flow) was accomplished through spectral filtering. For OH fluorescence, a combination of a 2mm thick WG-305 and a 1 mm thick UG-11 Schott colored glass filters was used. For detecting NO, an Andover narrow band interference filter with a bandpass of 8 nm FWHM and a peak transmittance of 10% centered at 238 nm, was used. Wavelength selection is a critical consideration for NO detection, in order to avoid the Schumman-Runge band system of O_2 which overlaps much of the NO spectrum at elevated pressures and temperatures.[10] An Andover narrow band interference filter provided selective detection of C_2. This filter had a peak transmittance of 64% centered at 532.4 nm with a bandpass of 2.9 nm FWHM.

FLAMETUBE HARDWARE

The sector hardware used in this study has been described previously[11] but a brief description is provided here. A sector is a subsection of a full annular combustor. Due to the expense of building a full combustor, initial tests are conducted on an arc containing several adjacent fuel injector assemblies. Sectors are used to assess interactions between potential combustor elements, particularly fuel injectors. While most sectors are true arcs, the one used for this study had a rectangular cross section, thereby greatly simplifying the implementation of laser diagnostics. Due to the proprietary nature of this fuel injector design, no detailed written or schematic description can be provided.

Figure 3 shows a schematic of the optically accessible sector combustor. The stainless steel (SS) housing is lined with a cast ceramic material and is water-cooled. The inlet flow path area measures 8.5 in x 8.5 in (21.6 cm x 21.6 cm). Within this area three fuel injector "domes" are fitted. The dome refers to the area in the combustor in which the primary combustion air and fuel are introduced. Each dome consists of an array of identical fuel injectors. The outer domes (bottom and top) in this radially staged combustor are composed of lean premixed prevaporized (LPP) injectors, while the center dome contains the pilot injectors, which operate as partially premixed swirl-stabilized fuel-air mixers. Two arrangements of the domes are possible. In the first, or the "staggered" configuration, the exit plane of the center dome is in its upstream position, approximately 1.8 in (4.6 cm) ahead of the exit plane of the outer domes. In the second, configuration, referred to for the purposes of this report as the "flush" position, the center dome is located farther downstream with its exit plane approximately 0.71 in (1.8 cm) ahead of that of the outer domes. Further downstream, the chamber necks down to an exhaust area measuring 4.0 in (10.2 cm) high x 8.0 in (20.4 cm) wide. To allow simultaneous gas analysis of the flow, radially mounted sample extraction probes are located in this smaller exit region.

Optical accessibility is achieved through a window design described in detail elsewhere.[12] The UV grade fused silica windows measuring 1.5 in (3.8 cm) axially, 2.0 in (5.1 cm) in the direction normal to the flow and 0.5 in (1.3 cm) thick, are positioned so that the exit plane of the top dome can be seen. The top and bottom windows are centered with respect to the rig centerline. The side windows however, are offset 1.0 in (2.5 cm) above the rig centerline in order to center the field of view of these windows on the interface region between the upper and pilot domes. Figure 4 shows the window positions with the respective fields

of view for each of the two sector rig configurations. Also shown are the laser sheet positions for horizontal and vertical insertion. Laser sheet positions were typically 0.2 in (5 mm) apart resulting in a total of 9 possible positions ranging from +0.8 in to -0.8 in (+20 mm to -20 mm). Zero positions were the rig centerline for vertical laser sheet insertion, and the interface between the pilot dome and the upper dome for horizontal laser sheet insertion. To keep the windows from experiencing thermal damage, they were thin-film cooled. The nitrogen gas cooling provided no more than 12% of the aggregate combustor mass flow rate, which, for this series of experiments, did not exceed 4.10 kg/s.

RESULTS AND DISCUSSION

For the images presented herein, no signal processing routines such as background subtraction, normalization for laser sheet energy distribution, or corrections for shot-to-shot variations in laser energy were performed. The data was subjected to smoothing and scaling routines to render the images free of noise spikes and to enhance legibility. All images, unless otherwise specified, were acquired as a series of five single-shot images. However, some on-chip averages, in which a pre-determined number of images are stored and integrated on the imaging chip, were acquired for selected points. In all images the flow is from left to right. The gray scale to the left of each Figure shows the relative signal intensities increasing from bottom to top.

OH IMAGING

The doubled dye output was tuned to specific rovibronic transitions of the OH (1,0) band, namely $R_1(10)$, $R_1(11)$, and $R_1(12)$ at 281.607 nm, 281.824 nm, and 282.055 nm, respectively. These bands were found previously to have little or no attenuation across similarly constituted flows.[6] The laser energy was maintained at approximately 16 mJ for each of these wavelengths.

Figure 5 shows typical single shot PLIF images obtained with the radially-staged sector combustor in the staggered configuration. The OH $R_1(10)$ excitation wavelength was used with horizontal laser sheet insertion at +20 mm (top sequence) and -20 mm (bottom sequence). This Figure serves to make two points: 1) There are significant differences between the imaged flowfields arising from the two types of fuel injectors examined within the image (LPP top, pilot bottom); and 2) There is considerable shot-to-shot variation in the flow field at both laser sheet insertion points. The top sequence shows little interaction between adjacent LPP injectors, which was found in every image obtained at this location. The image sequences in the Figure show that PLIF can also be quite useful in differentiating flow structure characteristic of different fuel injector types.

The optimum number of laser shots necessary to best characterize the flowfield in the radially-staged sector combustor was determined. This examination found, after looking at images obtained with numbers of shots ranging from 1 to 600, that 25 laser shots were adequate to typify the flow for any given laser sheet insertion point.

Figure 6 shows a comparison between resonant $R_1(11)$ and non-resonant (281.824 nm) OH excitation for the sector at identical flow conditions in the "flush" configuration with vertical laser sheet insertion. As in Figure 5, the dominant feature in both cases is the intense signal immediately downstream of the LPP injectors. Clearly the fluorescence from this region has a significant "noise" contribution. The non-resonant signal is essentially equivalent to the resonant signal in this region. However, in the boxed lower region, there is two times more signal emanating from the pilot region for the resonant case than in the non-resonant case. The boxed region in both images was processed independent of the remaining image to enhance the signals. Once this was accomplished, the remaining image was scaled so that its maximum pixel value was equal to the maximum pixel value of the boxed region. The rationale for this action is that the emission emanating from the excited LPP effluent is so much stronger than that from the lower region (on the order of 4 to 5 times greater), that in order to examine both areas simultaneously, the lower region must be processed separately. Plainly, the majority of the resonant signal in the pilot region is from OH fluorescence, while that downstream of the LPP injectors is strongly influenced by interfering emissions.

A comparison of images for a range of equivalence ratios (ϕ = 0.44, 0.49, 0.51, and 0.57) is shown in Figure 7. This sequence was collected using vertical OH $R_1(12)$ laser sheet insertion with the sector rig in the "flush" configuration. Again, as in Figure 6, the lower region has been enhanced for better visibility of the OH signal. These images, all taken at the zero position, show the flowfield under the same inlet conditions of temperature (739 K) and pressure (14.3 atm). As expected for fuel-lean cases, the OH fluorescence intensity increases with increasing equivalence ratio.

FLUORESCENCE INTERFERENCE

Earlier studies comparing resonant and non-resonant OH excitation in single injector flame tubes were relatively free of fluorescence interferences.[6] This observation was attributed largely to the window location, which was well downstream of the primary reaction zone. The window location on this radially-staged sector rig, however, intersects the area immediately downstream of the LPP fuel injectors. The signal observed at this location in the previous Figures is attributed primarily to PAH fluorescence, based upon the results obtained from the resonant and non-resonant laser excitation comparison. Fluorescence interferences attributed to PAH's (using similar laser fluences as this study) have been reported from the fuel-rich, high temperature zone of heptane-fueled spray flames.[13] That study examined PAH's that were formed in a region containing fuel vapor, combustion intermediates and pyrolysis products. In the present study however, due to the fuel-lean conditions and the window location, there may not be adequate time for PAH formation to occur; therefore the fluorescence that is being observed in the region immediately downstream of the LPP injectors must originate not only from OH but from other molecular species present in the fuel. The JP-5 fuel can, on a volumetric basis, contain up to 25% aromatics with a large fraction of these being PAH.[14] Due to this interference, exclusive observation of OH fluorescence in this region is clearly made more problematic.

Initial experiments have been performed using a narrow band interference filter centered at 315.1 nm with a 2.3 FWHM and 9.0% transmission efficiency. A comparison of resonant and non-resonant images downstream of the LPP injectors in the staggered configuration shows a drastic 85% reduction in fluorescence intensity in the non-resonant case. This result shows that selective spectral filtering may be an efficient means to discriminate between the broadband PAH emissions and the OH fluorescence in regions where both are present.

NO IMAGING

Figure 8 presents NO PLIF data acquired with the pilot in the upstream position for a range of equivalence ratios. The excitation wavelength was 225.386 nm, with the laser sheet in the vertical orientation. Each image frame is a 600 laser-shot on-chip average. To eliminate possible fluorescence interference in the LPP downstream region, only the signal within the boxes of each image in Figure 8 is analyzed. With the exception of the drop between ϕ = 0.54 and ϕ = 0.57, a rise in fluorescence signal was seen with increasing equivalence ratio. This drop might be attributed to some local flow anomaly causing a decrease in the local NO concentration at the time the image was acquired. To support this hypothesis, the data coincidentally acquired by gas sample extraction probes is presented in Figure 9.

As is clearly evident in this comparison of the gas sampled NO_x signal with the NO PLIF data, the NO_x gas sampled data reproduces nearly point-for-point the NO PLIF data, showing the same drop in NO concentration occurring between ϕ = 0.54 and ϕ = 0.57. The signal in the boxed region is clearly due to NO fluorescence since in fuel-lean combustion, as equivalence ratio increases additional fuel is added leading to greater O_2 consumption. This results in a higher flame temperature and subsequently increased NO formation. From these factors we conclude that the observed increase in fluorescence intensity with increasing equivalence ratio is due to NO formation. The results presented by Figures 8 and 9 clearly demonstrate the value of the PLIF technique as a diagnostic tool for planar detection of low concentrations of NO in complex combustion flowfields.

C_2 IMAGING

Imaging the chemiluminescence emanating from nascent C_2 in the flow provides an opportunity to investigate the region immediately downstream of the pilot dome, which is inaccessible to laser excitation. An image capturing C_2 Chemiluminescence is shown in Figure 10. For this image the camera was focused at the vertical zero position. This image, with the pilot in the staggered configuration, clearly shows that the C_2 fluorescence sweeps from the pilot region into the LPP injector dome region. This motion is indicative of the presence of a recirculation zone in this interface region between the two domes. Also evident is the lack of any apparent C_2 in the downstream area of the pilot dome beyond this interface region. This is supported by the observation in Figure 6 comparing resonant and non-resonant OH fluorescence which showed the almost complete absence of any interfering PAH fluorescence in this region.

SUMMARY AND CONCLUSIONS

This preliminary study has presented PLIF images of combustion species within a JP-5 burning, radially-staged sector combustor operating at conditions of high pressures and temperatures. PLIF images using resonant OH excitation wavelengths were acquired for several different injector dome configurations. These images displayed the nearly total lack of interaction between individual LPP injectors in the upper dome. OH PLIF imaging immediately downstream of the LPP fuel injectors was found to be problematic at these conditions due to the higher percentage of interfering PAH fluorescence. However, comparison of images obtained using resonant and non-resonant OH excitation allowed the fluorescence collected downstream of the pilot dome to be attributed to OH. The images obtained in this study indicate that OH PLIF is an excellent tool to identify flow characteristics arising from diverse fuel injector types. PLIF imaging of PAH could serve as a diagnostic to identify situations in which there is low fuel flow to the injectors or the presence of fuel line or injector obstruction. Recent investigations have indicated that narrow band spectral filtering could be highly effective at abating broadband PAH emissions.

The first ever NO PLIF images at these conditions were captured for a variety of equivalence ratios and compared favorably to simultaneously acquired gas sample extraction data. These results point to the soundness of using PLIF as a diagnostic for attaining two-dimensional mapping of low concentrations of NO at actual operating conditions.

Images of nascent C_2 radical chemiluminescence were also obtained. These data showed the flow in a region inaccessible to laser probing. Additionally, C_2 imaging displayed the interactions between the pilot and the LPP domes denoting the need to perform a more in-depth study of the complex recirculation phenomenon present in these types of combustors.

Images such as presented here serve to detail individual fuel injector performance as well as reveal interactions, or lack thereof, between juxtaposed fuel injectors and injector domes. These images, presently unattainable elsewhere, give researchers a valuable opportunity to observe and assess engine subcomponents at actual working conditions.

Future work is planned in which a second ICCD camera will be used to capture a simultaneous laser sheet profile for use in normalizing the fluorescence PLIF image for variations in the laser sheet energy distribution. An investigation will also be made to examine alternative spectral filtering techniques in an attempt to reduce or eliminate fluorescence interferences. Additionally, the sector rig design allows for the fuel injection domes to be shifted further upstream. This would allow interrogation of the post combustion region farther downstream of the LPP injectors, presumably free of interfering fluorescence from PAH's. Finally, further investigations will be made to determine the detection limitations and the extent to which the NO PLIF measurements can be quantified.

ACKNOWLEDGMENTS

The Authors would like to acknowledge Wade Arida, Jeffery Bobonik, Dean Kocan, Bob McCluskey, Joe Morgan, and Ray Williams, for their many contributions in conducting this study.

REFERENCES

1. Eckbreth, A. C., *Laser Diagnostics for Combustion Temperature and Species*, and references cited therein, Abacus Press, Cambridge, MA, (1988).

2. Kohse-Höinghaus, K., "Quantitative Laser-Induced Fluorescence: Some Recent Developments in Combustion Diagnostics," *Appl. Phys. B*, **50**, pp. 455-461, 1990.

3. Hanson, R. K., "Combustion Diagnostics: Planar Imaging Techniques," *Twenty-first Symposium (International) on Combustion*, Combustion Institute, Pittsburgh, pp. 1677-1691, 1986.

4. Allen, M. G., McManus, K. R., and Sonnenfroh, D. M., "PLIF Imaging in Spray Flame Combustors at Elevated Pressure," AIAA Paper 95-0172, 33rd Aerospace Sciences Meeting and Exhibit, Reno, NV, 1995.

5. Andresen, P., Meijer, G., Schluter, H., Voges, H., Koch, A., Hentschel, W., Oppermann, W., and Rothe, E., "Fluorescence Imaging Inside an Internal Combustion Engine Using Tunable Excimer Lasers," *App. Opt.* **29**, (16), pp. 2392-2404, 1990.

6. Locke, R. J., Hicks, Y. R., Anderson, R.C., and Ockunzzi, K. A., "OH Imaging in a Lean Burning High-Pressure Combustor," *AIAA J.*, **34** (3), pp. 622-624, 1996.

7. Penner, S. S., Wang, C. P., and Bahadoria, M. Y., "Laser Diagnostics Applied to Combustion Systems," *Twentieth Symposium (International) on Combustion*, Combustion Institute, Pittsburgh, PA, pp. 1149-1176, 1984.

8. Wesoky, H. L. and Prather, M. J., "Atmospheric Effects of Stratospheric Aircraft," 10th International Symposium on Air Breathing Engines, Nottingham, England, pp. 211-220, 1991.

9. Whitehead, A. H., Jr., "First Annual High-Speed Research Workshop," *1st High-Speed Research Workshop*, Williamsburg, VA, 1992.

10. Partridge, W. P., Klassen, M. S., Thomsen, D. D., and Laurendeau, N. M., "Experimental Assessment of O_2 Interferences on Laser-Induced Fluorescence Measurements of NO in High-Pressure, Lean, Premixed Flames by Use of Narrow-Band and Broadband Detection," *App. Opt.*, **34** (24), pp. 4890-4904, 1996.

11. Hicks, Y. R., "Multi-Dimensional Measurements of Combustion Species in Flame Tube and Gas Sector Turbine Combustors," NASA TM 1073329, 1996.

12. Locke, R. J., Hicks, Y. R., Anderson, R. C., Ockunzzi, K. A., and North, G. L., "Two-Dimensional Imaging of OH in a Lean Burning High Pressure Combustor," NASA TM 106854, 1995.

13. Allen, M. G., McManus, K. R., and Sonnenfroh, D. M., "PLIF Imaging Measurements in High-Pressure Spray Flame Combustion," AIAA Paper 94-2913, 30th AIAA/ASME/SAE/ASEE Joint Propulsion Conference, Indianapolis, IN, 1994.

14. Coordinating Research Council, "Handbook of Aviation Fuel Properties," CRC Report Number 530, Coordinating Research Council, Inc., Atlanta, GA, 1983.

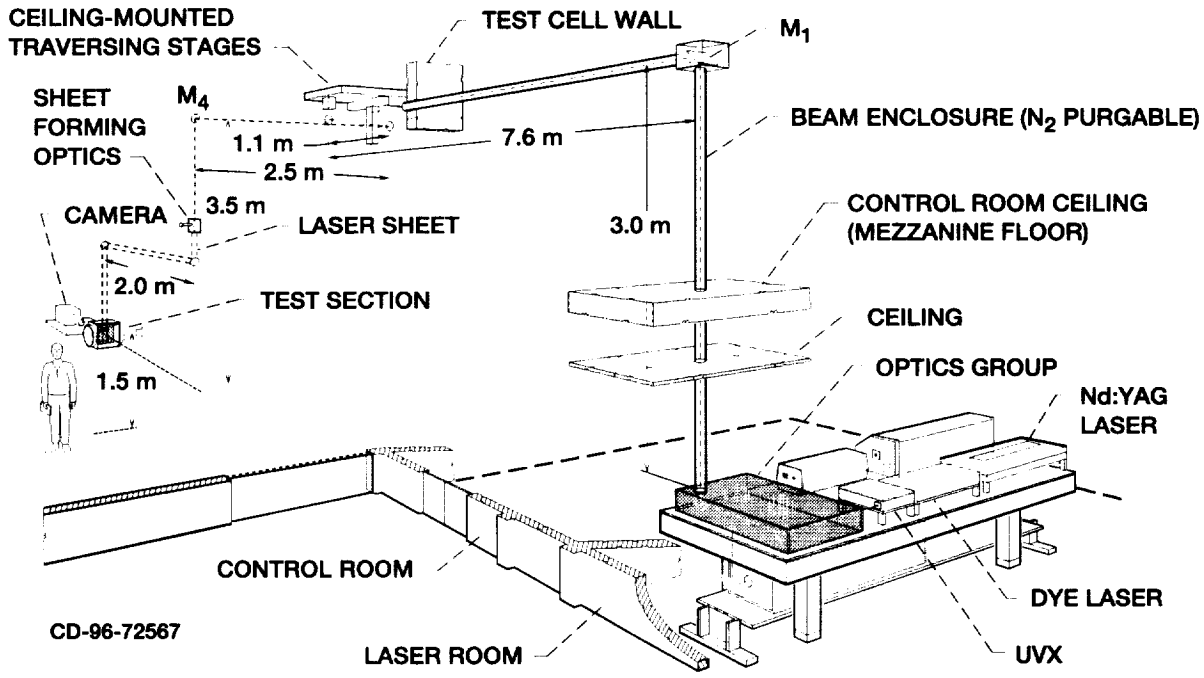

Figure 1. Laser beam delivery system.

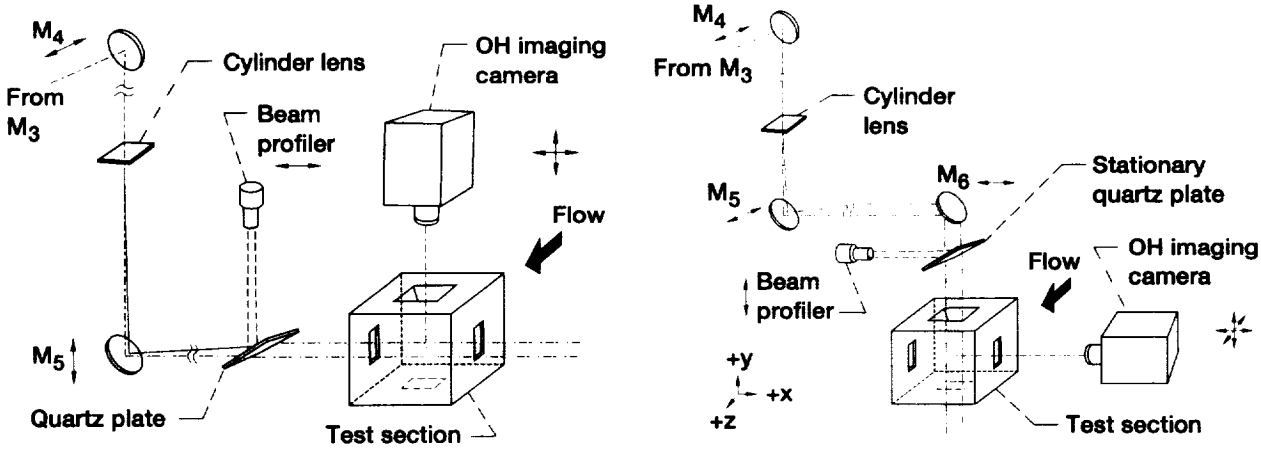

(a) Horizontal input beam.

(b) Vertical input beam.

Figure 2. Schematic representation detailing optical setup for horizontal (left) and vertical (right) laser sheet insertion.

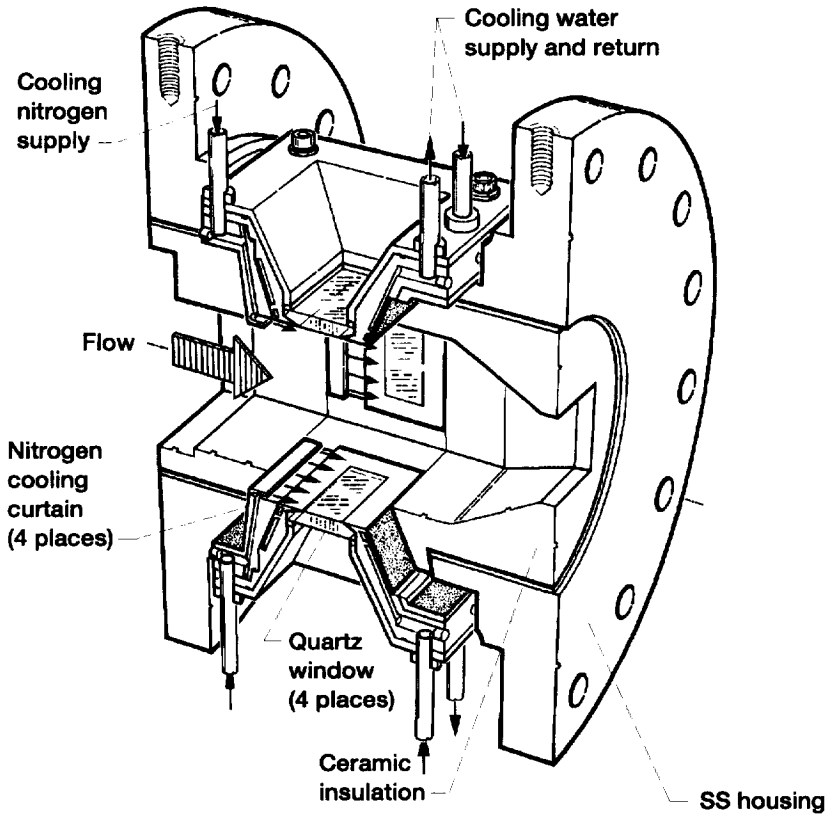

Figure 3. Sector combustion shell with quartz window assemblies.

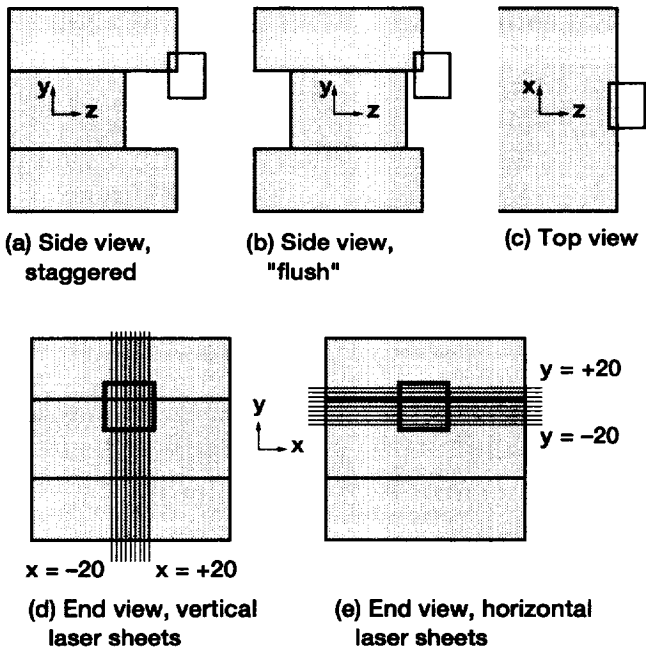

Figure 4. Window positions with fields of view for each sector configuration, including laser sheet positions for horizontal and vertical implementation.

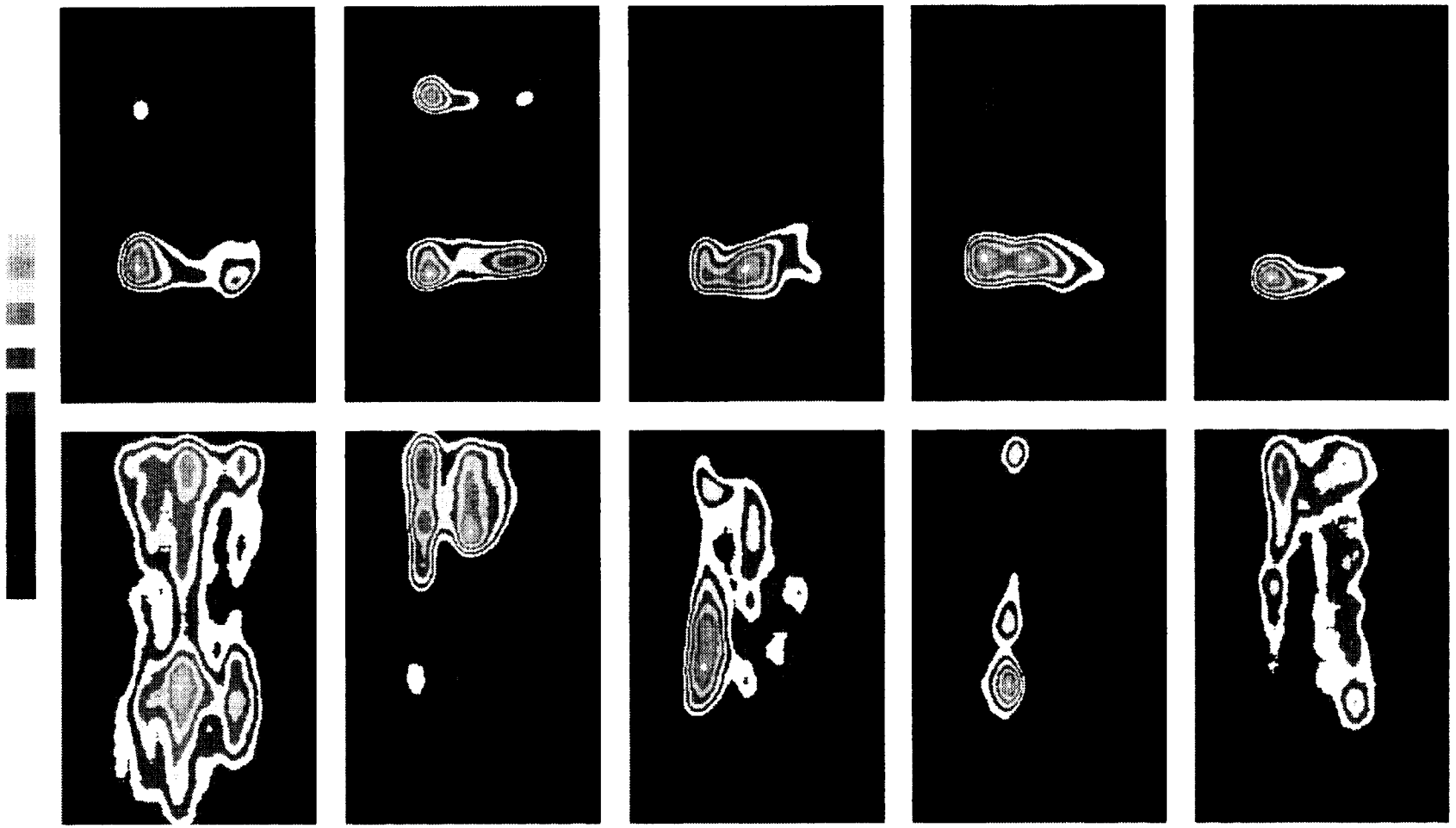

Figure 5. Shot-to-shot variation in flame structure for the staggered dome configuration, using horizontal laser sheet insertion. Resonant OH excitation is $R_1(10)$. T_{in} = 710K, P_{in} = 1020 kPa, ϕ=0.57. Laser sheet position - top row: +20 mm; bottom Row: -20 mm.

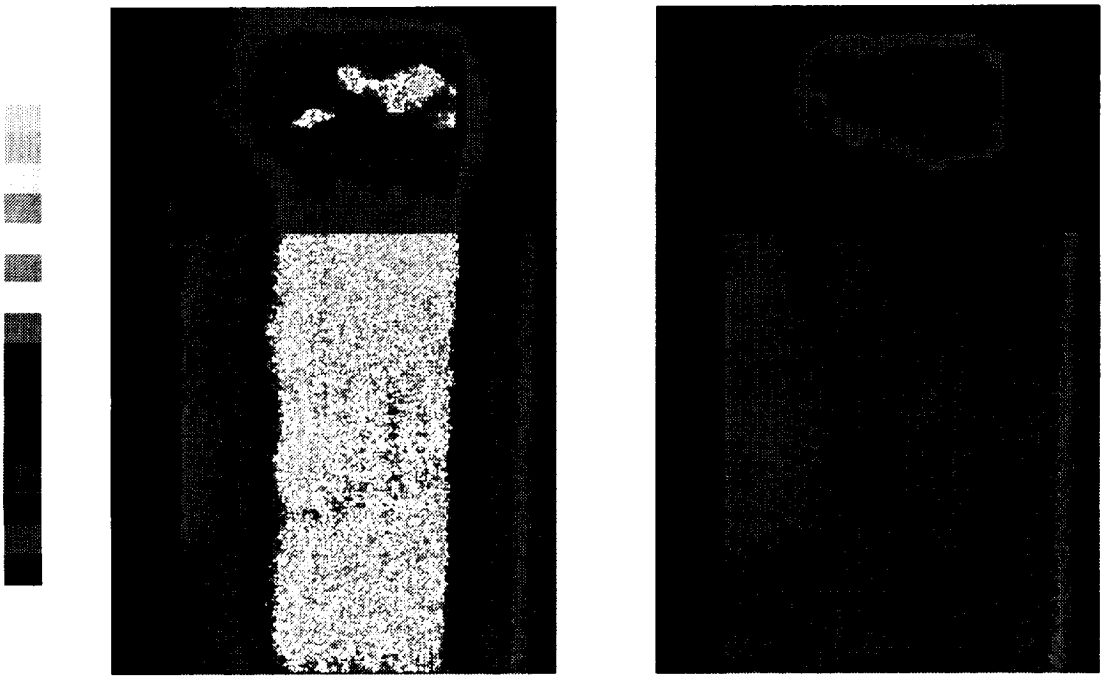

Typical Resonant Image
X=-10

Typical Non-resonant Image
X=-10

Figure 6. Image comparison in the staggered dome configuration for resonant (left) and non-resonant (right) OH excitation, using vertical laser sheet insertion. Resonant excitation is $R_1(11)$; non-resonant excitation is at λ = 281.824 nm. T_{in} = 833K, P_{in} = 910 kPa,and ϕ=0.44.

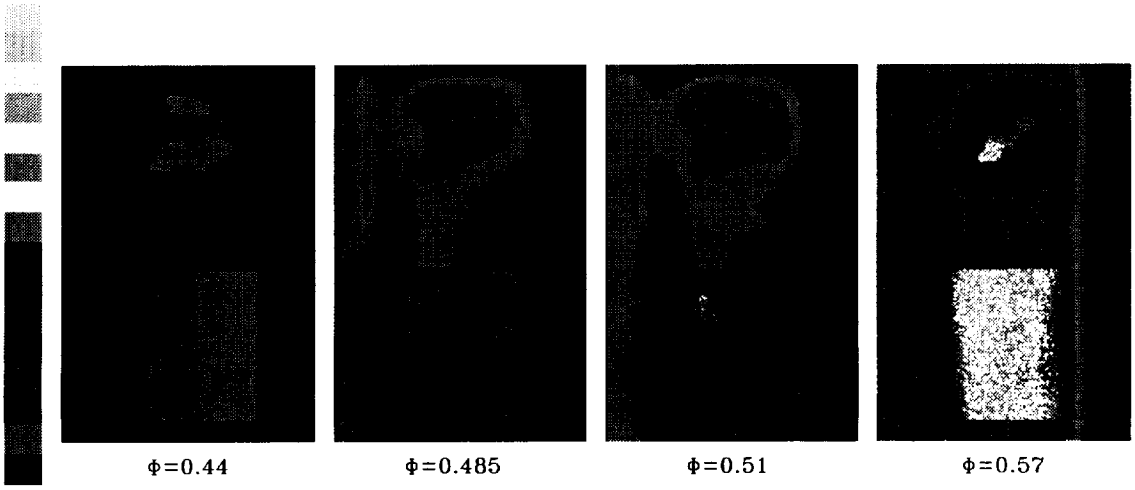

ϕ=0.44 ϕ=0.485 ϕ=0.51 ϕ=0.57

Figure 7. Comparison of OH PLIF images for increasing equivalence ratios in the "flush" dome configuration using a vertical laser sheet insertion at the zero position. T_{in} = 739K, P_{in} = 1450 kPa. Resonant excitation is $R_1(12)$.

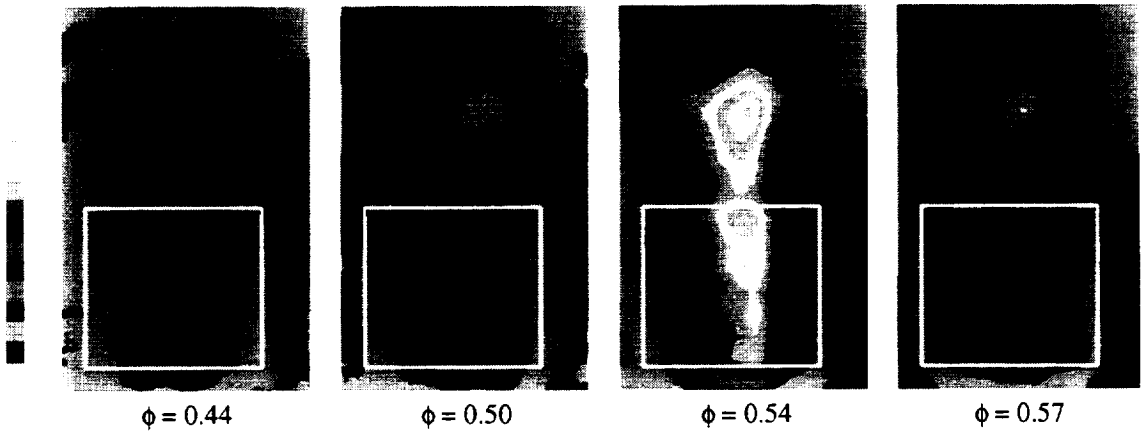

Figure 8. Comparison of NO PLIF images for increasing equivalence ratios in the staggered dome configuration using vertical laser sheet insertion at the zero position. T_{in} = 833K. P_{in} = 910 kPa..

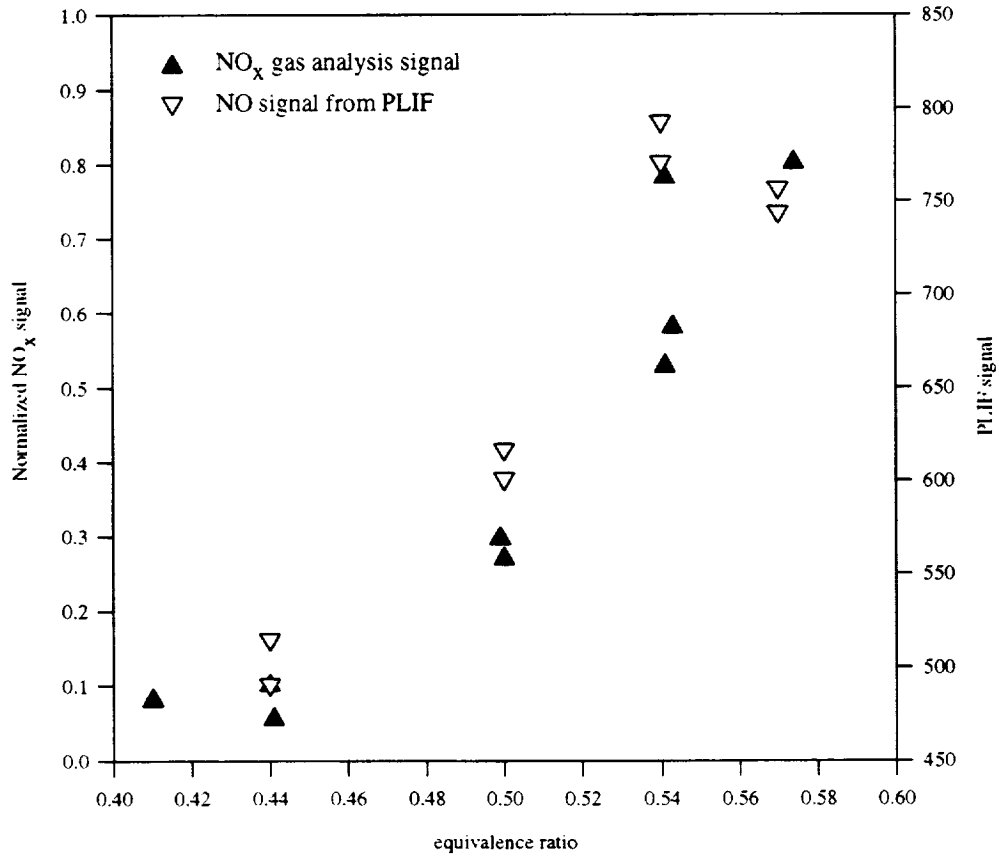

Figure 9. Graph showing a comparison of the NO PLIF data and the gas sampled NO_x data acquired in the staggered dome configuration. T_{in} = 833K. P_{in} = 910 kPa.

REPORT DOCUMENTATION PAGE

Form Approved
OMB No. 0704-0188

1. AGENCY USE ONLY (*Leave blank*)	2. REPORT DATE	3. REPORT TYPE AND DATES COVERED
	December 1996	Technical Memorandum

4. TITLE AND SUBTITLE

Imaging of Combustion Species in a Radially-Staged Gas Turbine Combustor

5. FUNDING NUMBERS

WU-537-05-20

6. AUTHOR(S)

Randy J. Locke, Yolanda R. Hicks, Robert C. Anderson,
Kelly A. Ockunzzi, and Harold J. Schock

7. PERFORMING ORGANIZATION NAME(S) AND ADDRESS(ES)

National Aeronautics and Space Administration
Lewis Research Center
Cleveland, Ohio 44135-3191

8. PERFORMING ORGANIZATION REPORT NUMBER

E-10542

9. SPONSORING/MONITORING AGENCY NAME(S) AND ADDRESS(ES)

National Aeronautics and Space Administration
Washington, DC 20546-0001

10. SPONSORING/MONITORING AGENCY REPORT NUMBER

NASA TM-107373

11. SUPPLEMENTARY NOTES

Prepared for the 33rd Joint Combustion and Propulsion Systems Hazards Subcommittees Meeting sponsored by the Joint Army-Navy-NASA-Air Force Interagency Propulsion Committee, Monterey, California, November 4–9, 1996. Randy J. Locke, NYMA, Inc., 2001 Aerospace Parkway, Brook Park, Ohio 44142 (work funded by NASA Contract NAS3–27186); Yolanda R. Hicks and Robert C. Anderson, NASA Lewis Research Center; Kelly A. Ockunzzi, Case Western Reserve University, Computer Engineering Department, Cleveland, Ohio 44106; Harold J. Schock, Michigan State University, Mechanical Engineering Department, East Lansing, Michigan 48864. Responsible person, Yolanda R. Hicks, organization code 5830 (216) 433–3410.

12a. DISTRIBUTION/AVAILABILITY STATEMENT

Unclassified - Unlimited
Subject Category 07

This publication is available from the NASA Center for AeroSpace Information, (301) 621–0390.

12b. DISTRIBUTION CODE

13. ABSTRACT ***(Maximum 200 words)***

Planar laser-induced fluorescence (PLIF) is used to characterize the complex flowfield of a unique fuel-lean, radially-staged, high pressure gas turbine combustor. PLIF images of OH are presented for two fuel injector configurations. PLIF images of NO, the first acquired at these conditions, are presented and compared with gas sample extraction probe measurements. Flow field imaging of nascent C_2 chemiluminescence is also investigated. An examination is made of the interaction between adjoining lean premixed prevaporized (LPP) injectors. Fluorescence interferences at conditions approaching 2000 K and 15 atm are observed and attributed to polycyclic aromatic hydrocarbon (PAH) emissions. All images are acquired at a position immediately downstream of the fuel injectors with the combustor burning JP–5 fuel.

14. SUBJECT TERMS	15. NUMBER OF PAGES
Laser diagnostics; PLIF; Combustion; OH	15
	16. PRICE CODE: A03

17. SECURITY CLASSIFICATION OF REPORT	18. SECURITY CLASSIFICATION OF THIS PAGE	19. SECURITY CLASSIFICATION OF ABSTRACT	20. LIMITATION OF ABSTRACT
Unclassified	Unclassified	Unclassified	

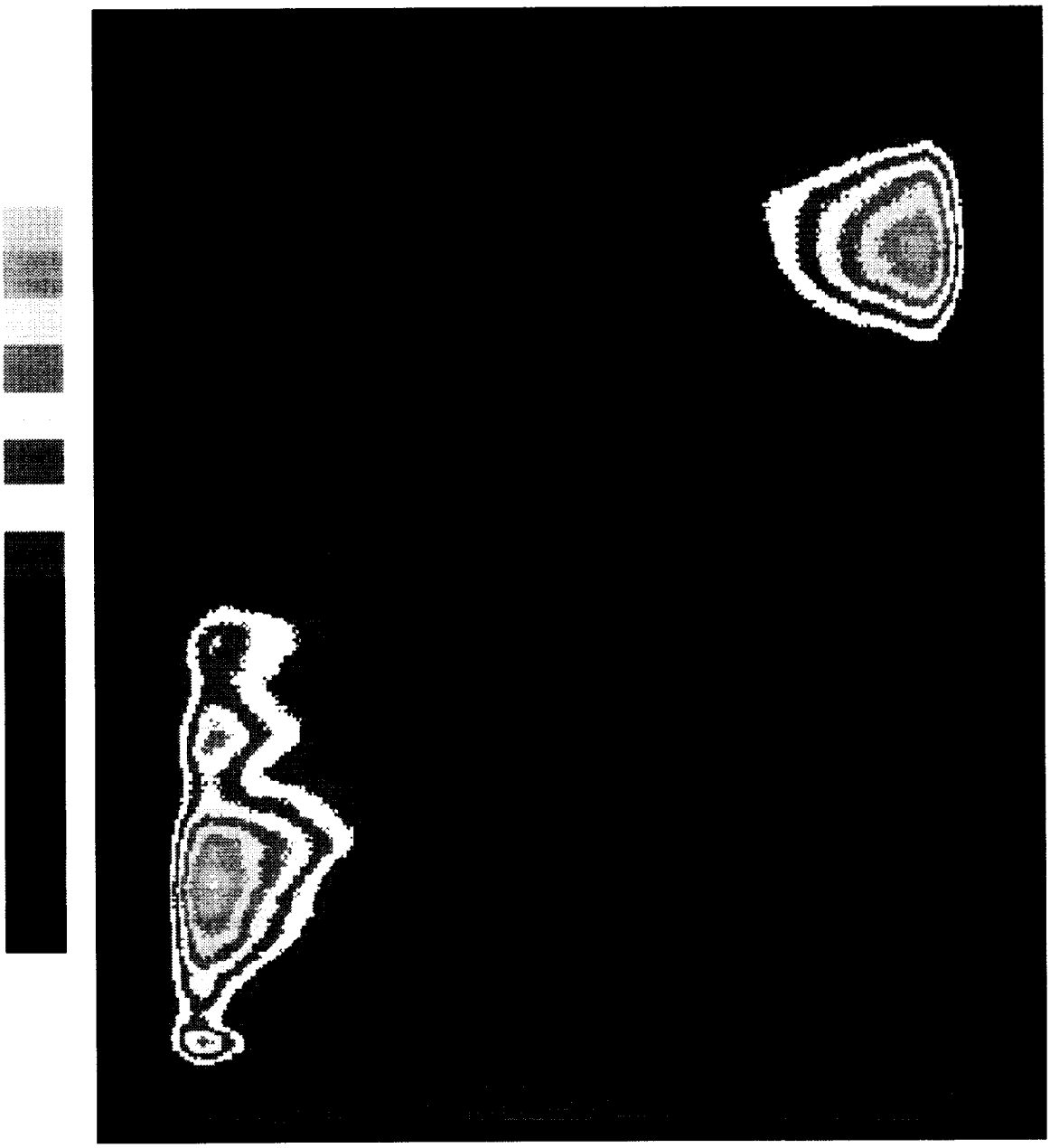

Figure 10. Image of naturally occurring fluorescence from C_2 at 532 nm with the dome in the staggered configuration. T_{in} = 730K, P_{in} = 950 kPa. and Φ = 0.43.